Transverse Single-Spin Asymmetry for Inclusive and Diffractive Electromagnetic Jets at Forward Rapidities in $p^{\uparrow}+p$ collisions at $\sqrt{s} = 200$ GeV and 500 GeV at STAR

Xilin Liang[1] (for the STAR Collaboration)

[1]University of California at Riverside, Riverside, CA 92521, USA

Abstract

There have been numerous attempts, both theoretical and experimental, to understand the origin of the unexpectedly large transverse single-spin asymmetry (A_N) for the inclusive hadron production at forward rapidities observed in $p^{\uparrow}+p$ collisions at various center-of-mass energies. The twist-3 contributions in the collinear factorization framework and the transverse-momentum-dependent contributions from the initial-state quark and gluon Sivers functions and/or final-state Collins fragmentation functions are potential explanations. In addition, previous analyses of A_N for forward π^0 and electromagnetic jets in $p^{\uparrow}+p$ collisions at STAR indicated that there might be non-trivial contributions to the large A_N from diffractive processes. To investigate the underlying physics regarding large A_N, we study the A_N for electromagnetic jets (EM-jets) produced in inclusive processes with the STAR Forward Meson Spectrometer (FMS) using $p^{\uparrow}+p$ data at $\sqrt{s} = 200$ GeV and 500 GeV. These results are consistent with the previously published results and provide rich information for understanding the physics mechanism for large A_N. Also, the new preliminary results of the A_N for EM-jets in diffractive processes using the FMS with $\sqrt{s} =$ 200 GeV data are presented. We observe non-zero A_N for the diffractive EM-jets and with the opposite sign compared to the inclusive EM-jets A_N. Further theory inputs are needed to understand diffractive EM-jet results.

1 Introduction

Transverse single-spin asymmetries, which are defined as left-right asymmetries of the particle production with respect to the plane defined by the momentum and spin directions of the polarized beam, have been observed to be large for charged- and neutral-hadron production in hadron-hadron collisions over a couple of decades [1, 2, 3, 4, 5]. In pQCD, however, the A_N is predicted to be small and close to zero in high energy collisions [6]. There are two major frameworks that can provide a potential explanation for such sizeable asymmetries. The first one is the transverse-momentum-dependent (TMD) contributions from the initial-state quark and gluon Sivers functions and/or the final-state Collins fragmentation functions. In the Sivers mechanism, the asymmetry comes from the correlation between the proton spin and the parton transverse momentum [7], while the Collins effect arises from the correlation between the spin of the fragmenting quark and the outgoing hadron's transverse momentum [8]. Another framework is based on the twist-3 contributions in the collinear factorization framework, including the quark-gluon or gluon-gluon correlations and fragmentation functions [9]. In addition, previous analyses of A_N for forward π^0 and electromagnetic jets (EM-jets) in $p^{\uparrow}+p$ collisions at STAR indicated that there might be non-trivial contributions to the large A_N from diffractive processes [5].

We present the results for A_N of inclusive EM-jets using $p^{\uparrow}+p$ collisions at $\sqrt{s} = 500$ GeV and 200 GeV at STAR. In addition, we present the preliminary results for the dependence of A_N on photon multiplicity inside the EM-jet, EM-jet transverse momentum (p_T) and energy using $p^{\uparrow}+p$ collisions at $\sqrt{s} = 200$ GeV. Lastly, we present the new preliminary results for A_N of diffractive EM-jets using $p^{\uparrow}+p$ collisions at $\sqrt{s} = 200$ GeV.

2 Analysis

2.1 Experiments

The measurements have been performed with the STAR detector at Relativistic Heavy Ion Collider (RHIC) at Brookhaven National Laboratory. RHIC is the only polarized proton-proton collider in the world, which can provide transversely or longitudinally polarized proton-proton collisions at $\sqrt{s} = 200$ GeV and 500/510 GeV. The data sets used are the transversely polarized $p^{\uparrow}+p$ collisions at $\sqrt{s} = 500$ GeV and 200 GeV collected in 2011 and 2015 at STAR, with average beam polarizations about 52% and 57% and integrated luminosities of 25 pb^{-1} and 52 pb^{-1}, respectively.

The analyses use the Forward Meson Spectrometer (FMS) to reconstruct photons and the Roman Pots (RP) for tagging diffractive processes with slightly scattered protons close to the beamline. The FMS is an electromagnetic calorimeter used to detect photons, neutral pions, and eta mesons, with

the pseudo-rapidity coverage of 2.6 - 4.2 and the full azimuthal coverage. There are 1264 lead-glass cells with photomultiplier tubes for readout. Each cell has more than 18 radiation length, which is long enough for incident photons to deposit sufficient energies for detection [10]. The RP detectors are located close to the beamline but about 15.8 meters away from the interaction point at both the east and west sides of the main STAR apparatus. They are vessels that house the Silicon Strip Detector planes (SSDs). On both sides, there are two sets of RP, separated by about 1.8 meters. Each RP set contains a package with 4 SSDs both above and below the beamline [11].

2.2 Electromagnetic jets reconstruction and corrections

The EM-jets are the EM component of the full jets. Their constituents, photon candidates, are FMS clusters, which are formed by grouping adjacent towers with non-zero energies. The photon candidates are required to have a minimum energy of 1 GeV. The EM-jets are reconstructed with the anti-k_T algorithm from the FastJet package [12], with the resolution parameter R = 0.7. More details about the analysis procedures can be found in [5].

The reconstructed jet energy and p_T are corrected by subtracting the contributions from the underlying events (UE), which are estimated using the "off-axis" cone method [13].

In addition, the Monte Carlo (MC) simulation events using PYTHIA 6.428 event generator with Perugia 2012 Tune are generated and then propagated through the GEANT-based STAR detector simulation to simulate the detector response. The jet kinematics are further corrected back to the "particle level" based on the MC simulation.

2.3 Event selection for the inclusive process

The possible channel for inclusive EM-jet production is $p^{\uparrow} + p \rightarrow EM - jet + X$, where the EM-jets are reconstructed from FMS. The EM-jet reconstruction is described in Sec. 2.2. The UE correction and energy correction from MC simulation are applied for the EM-jets. Finally, the EM-jets are required to have p_T greater than 2 GeV/c.

2.4 Event selection for the diffractive process

The rapidity gap between the FMS and the RP allows to find diffractive EM-jets in the FMS by tagging the proton tracks in the RP. Therefore, two possible channels are considered for diffractive EM-jet process: $p^{\uparrow} + p \rightarrow p + EM - jet + X$ and $p^{\uparrow} + p \rightarrow p + p + EM - jet + X$. Both channels require exactly one proton detected in the RP on the FMS side (forward side). The former channel requires no proton on the backward side, while the latter channel requires to have exactly one proton on the backward side. The proton tracks detected in RP are required to hit at least 7 out of 8 SSDs and be within the geometric acceptance of RP.

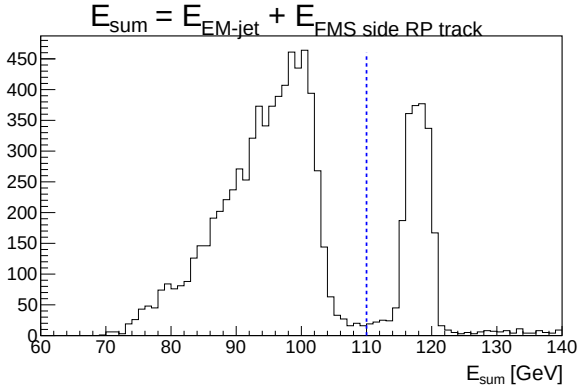

Figure 1: Distribution of sum energy of the EM-jet and the forward side proton track for the EM-jet x_F within [0.15, 0.2] in $p^{\uparrow}$ + p collisions at $\sqrt{s} = 200$ GeV. The blue dashed line separates the diffractive event candidates from accidental coincidences.

The EM-jet reconstruction for diffractive process is the same as described in Sec. 2.2. The EM-jets are required to have p_T greater than 1 GeV/c. The energy correction based on MC simulation is applied but the UE correction is not considered yet.

The selected diffractive events, however, contain large background, including pile-up events and the accidental coincidence. Therefore, two additional event selection criteria are applied to further suppress the background. The first cut is based on the sum of the EM-jet energy and the forward-side proton-track energy (sum energy), since the accidental coincident events usually have the sum energy greater than the proton beam energy. Figure 1 shows one example of the sum energy distribution for EM-jet x_F ranging from 0.15 to 0.2 in $p^{\uparrow} + p$ collisions at $\sqrt{s} = 200$ GeV. The Feynman-x is defined as $x_F = 2p_L/\sqrt{s}$, where p_L is the longitudinal momentum. For the EM-jet in FMS, x_F can be estimated by the EM-jet energy divided by the proton beam energy. The events from the left peak are accepted as the diffractive process events, while the events from the right peak are considered as accidental coincidences. The cuts for the sum energy vary in different x_F bins, which are listed in Table 1. The second cut is based on the Beam-Beam Counter (BBC), which is used for triggering, luminosity monitoring and local polarization measurement [16]. The events with ADC sum for small BBC tiles less than 100 and ADC sum for large BBC tiles less than 60 are kept. Those events with high BBC ADC sum are discarded since they are likely affected by pile-up.

2.5 Analysis method

The cross-ratio method is used to extract the A_N for both inclusive and diffractive processes, and the corresponding formulas are shown in Eq. (1) and (2). In both equations,

Table 1: Sum energy cut for different x_F bins

x_F	Sum energy [GeV]
[0.1, 0.15]	<108
[0.15, 0.2]	<108
[0.2, 0.25]	<110
[0.25, 0.3]	<110
[0.3, 0.45]	<115

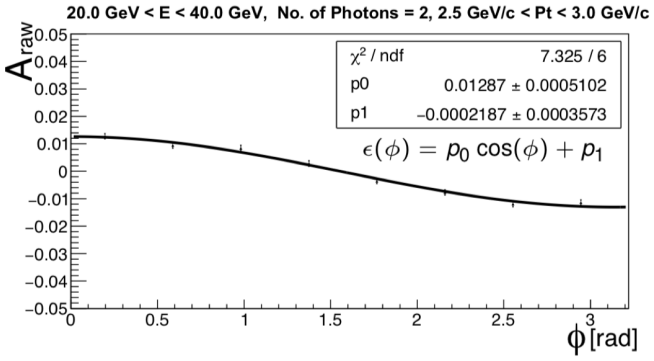

Figure 2: Example of fitting the raw asymmetry with $p_0\cos(\phi) + p_1$ for EM-jets with 2 photons, 20 GeV < E < 40 GeV and 2.5 GeV/c < p_T < 3.0 GeV/c.

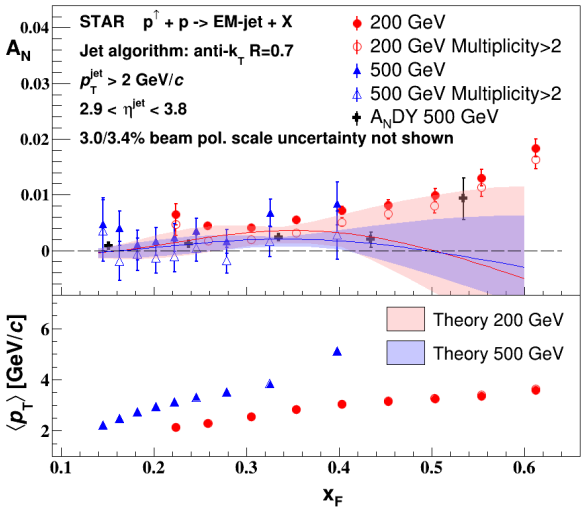

Figure 3: Transverse single-spin asymmetry as a function of x_F for EM-jets in transversely polarized proton-proton collisions at $\sqrt{s}$ = 200 GeV and 500 GeV [5]. The error bars show only the statistical uncertainties. The open symbols are the results for EM-jets consisting of more than two photons, while the solid symbols are the results for EM-jets without such a requirement. The theory curves are for A_N of full jets at 200 GeV and 500 GeV [14].

ϵ stands for the raw asymmetry. $N^{\uparrow(\downarrow)}(\phi)$, $N^{\uparrow(\downarrow)}(\phi+\pi)$ are the yields detected at ϕ, $(\phi+\pi)$ for spin up (down) state, where ϕ is the azimuthal angle of the EM-jet in the lab frame. P is the average polarization of the proton beam. The cosine fit is applied to extract the A_N from the raw asymmetry in Eq. (2). Figure 2 shows one example of the raw asymmetry as a function of ϕ and the cosine fit is applied to extract the A_N.

$$\epsilon = \frac{\sqrt{N^{\uparrow}(\phi)N^{\downarrow}(\phi+\pi)} - \sqrt{N^{\downarrow}(\phi)N^{\uparrow}(\phi+\pi)}}{\sqrt{N^{\uparrow}(\phi)N^{\downarrow}(\phi+\pi)} + \sqrt{N^{\downarrow}(\phi)N^{\uparrow}(\phi+\pi)}} \quad (1)$$

$$\epsilon = PA_N cos(\phi) \quad (2)$$

This method takes advantage of detector azimuthal symmetry and cancels effects due to the non-uniform detector efficiency and the time-dependent luminosity.

3 Results

3.1 Inclusive EM-jet A_N

Figure 3 shows the results for the inclusive EM-jet A_N as a function of x_F at 200 GeV and 500 GeV [5] along with the theory curves at those energies [14]. The A_N of the EM-jets increases with x_F. The 200 GeV results are significantly greater than zero, while the 500 GeV results are consistent with zero within uncertainty. In addition, the asymmetries in the overlap region of 200 GeV and 500 GeV indicate a weak energy dependence. The open symbols show the A_N with EM-jets consisting of more than 2 photons. They are smaller than the A_N without that requirement.

To further investigate the substructure dependence of inclusive A_N, a detailed analysis of photon multiplicity dependence of EM-jet A_N at forward rapidity using the FMS in $p^{\uparrow}$+p collisions at $\sqrt{s}$ =200 GeV is carried out. Figure 4 shows the EM-jet A_N as a function of x_F with 3 different photon multiplicity selections: $n_\gamma \leq 2$ (red solid point), $n_\gamma = 3$ (black solid point) and $n_\gamma \geq 4$ (blue open circle). The A_N generally increases with increasing x_F. It is observed that the A_N of EM-jets with 1 or 2 photons is larger than the A_N of the EM-jets consisting of 4 or more photons. This is consistent with the previous measurement [5], where the A_N of the isolated π^0 is higher than that of the non-isolated π^0.

Figure 5 shows the preliminary results of EM-jet A_N as a function of photon multiplicity, EM-jet p_T, and EM-jet energy using $p^{\uparrow} + p$ collisions at $\sqrt{s} = 200$ GeV. The asymmetries shown as black solid points are measured with respect to the polarized beam going into the FMS, which correspond to $x_F > 0$, while the asymmetries shown as red open circles are for $x_F < 0$, which correspond to the measurement with the polarized proton beam going in the opposite direction. For $x_F > 0$, the EM-jet A_N decreases with increasing photon multiplicity (jettiness). The EM-jets consisting of 1 or 2 photons have the strongest A_N, while the EM-jets consist-

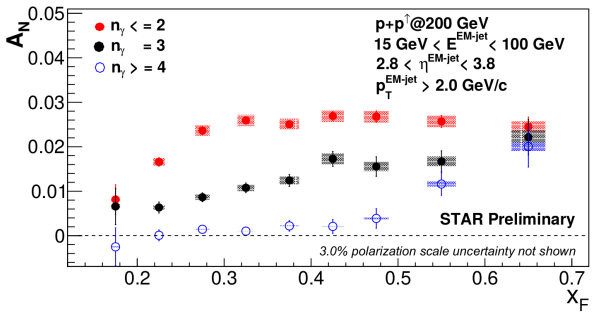

Figure 4: Transverse single-spin asymmetry as a function of x_F for EM-jets in transversely polarized proton-proton collisions at $\sqrt{s} = 200$ GeV for 3 different cases: $n_\gamma \leq 2$ (red solid point), $n_\gamma = 3$ (black solid point) and $n_\gamma \geq 4$ (blue open point). The systematic uncertainties (rectangular box) come from possible misidentification of event category.

ing of 4 or more photons have A_N close to 0. A_N for $x_F < 0$ is found to be consistent with 0 regardless of the jettiness. These results are consistent with the previous measurements at 500 GeV [15].

3.2 Diffractive EM-jet A_N

Figure 6 shows the preliminary results for diffractive EM-jet A_N as a function of x_F at $\sqrt{s} = 200$ GeV. To specify, the rightmost point is for $0.3 < |x_F| < 0.45$. The blue points are for $x_F > 0$. Those results show a non-zero A_N with 3.3σ significance from $A_N = 0$ line at forward rapidity. Also, large absolute A_N is observed at the high x_F region. However, the sign of the diffractive EM-jet A_N is negative, which is opposite to the inclusive EM-jet A_N shown in Fig. 3, Fig. 4 and Fig. 5. This sign change of A_N is an open question, which needs further theoretical inputs to be understood. In addition, the A_N for $x_F < 0$ is consistent with 0. The systematic uncertainty (the rectangular boxes) for A_N mainly comes from the event selections for suppressing the background events.

4 Conclusion

We present the inclusive EM-jet A_N using the FMS at STAR in $p^\uparrow + p$ collisions at $\sqrt{s} = 200$ GeV and 500 GeV. The A_N for inclusive EM-jets increases with increasing x_F. The consistency of A_N for both energies in the overlapping x_F region suggests a weak energy dependence. In addition, we study the A_N for EM-jets with different substructures using FMS at $\sqrt{s} = 200$ GeV. The A_N with higher jettiness is found to be smaller. Finally, we present the diffractive EM-jet A_N using the FMS at $\sqrt{s} = 200$ GeV. A non-zero A_N with a 3.3σ deviation from zero is observed and the A_N is large at high x_F region. However, the A_N is negative, which is opposite to inclusive A_N. Further theoretical inputs are needed to understand such a sign change. The presented STAR re-

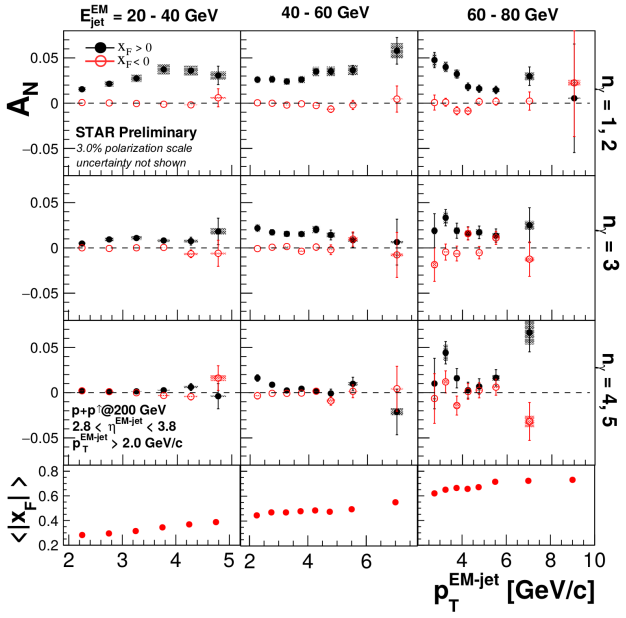

Figure 5: Transverse single-spin asymmetry for EM-jets in transversely polarized proton-proton collisions at $\sqrt{s} = 200$ GeV sorted by photon multiplicity, EM-jet energy and EM-jet p_T. The black solid points are for $x_F > 0$, while the red open circles are for $x_F < 0$. The lowermost panel shows the average x_F for each p_T bin. The systematic uncertainties (rectangular box) come from possible misidentification of event category.

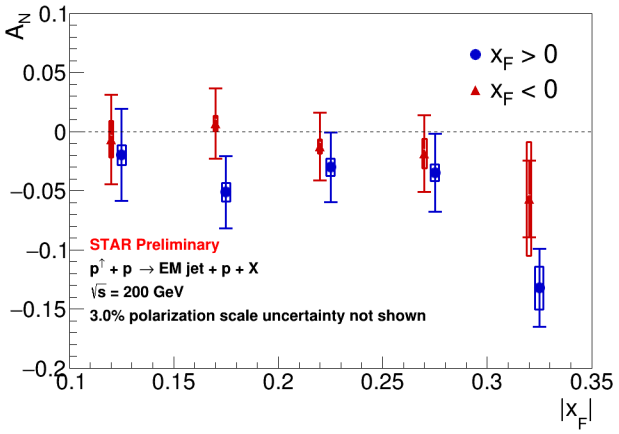

Figure 6: Transverse single-spin asymmetry for diffractive EM-jet as a function of x_F in transversely polarized proton-proton collisions at $\sqrt{s} = 200$ GeV. The blue points are for $x_F > 0$. The red points are for $x_F < 0$ with a constant shift of -0.005 along x-axis for clarity. The rightmost point is for $0.3 < |x_F| < 0.45$. The systematic uncertainty (the rectangular boxes) for A_N mainly comes from the event selections for suppressing the background events.

sults provide rich information for understanding the physics mechanism of large A_N in hadronic collisions.

5 Acknowledgement

The author is supported by the U.S. Department of Energy, Office of Science, Medium Energy Nuclear Physics program under award number DE-FG02-04ER41325.

References

[1] D.L. Adams *et al.*, Phys. Lett. B 261, 201(1991)
[2] B. I. Abelev *et al.* (STAR Collaboration), Phys. Rev. Lett. 101, 222001(2008)
[3] A. Adare *et al.* Phys. Rev. D 90, 012006 (2014)
[4] E.C. Aschenauer *et al.*, arXiv:1602.03922
[5] J. Adam *et al.* (STAR Collaboration), Phys. Rev. D 103, 092009 (2021)
[6] G. L. Kane, J. Pumplin, and W. Repko. Phys. Rev. Lett. 41, 1689 (1978)
[7] D. Sivers, Phys. Rev. D 41, 83 (1990)
[8] J. Collins, Nucl Phys B 396 (1993) 161
[9] J.W. Qiu and G. Sterman, Phys. Rev. Lett. 67 2264 (1991)
[10] J. Adam *et al.* (STAR Collaboration), Phys. Rev. D 98, 032013 (2018)
[11] J. Adam *et al.* (STAR Collaboration), Phys. Lett. B 808 (2020) 135663
[12] M.Cacciari, G. P. Salam, and G. Soyez, Eur. Phys. J. C (2012) 72: 1896
[13] B. B. Abelev *et al.* (ALICE Collaboration), Phys. Rev. D 91, 112012 (2015)
[14] L. Gamberg, Z. Kang, A. Prokudin, Phys. Rev. Lett. 110 23 232301 (2013)
[15] M.M. Mondal (STAR Collaboration) PoS (DIS2014) 216
[16] C. A. Whitten Jr. (STAR Collaboration), AIP Conference Proceedings 980, 390 (2008)